CFD SIMULATIONS FOR SOLAR COLLECTORS INCLUDING CONDENSATION AND ICE ACCRETION

Gernot J. Pauschenwein[1*]**, Christoph Reichl**[1]**, Bernd Windholz**[1]**, Immacolata Moretti**[1]**, and Michael Monsberger**[1]

[1] Austrian Institute of Technology, Energy Department, Sustainable Thermal Energy Systems, Giefinggasse 2, 1210 Vienna, Austria

* Corresponding Author, gernot.pauschenwein@ait.ac.at

Abstract

Nucleation processes such as condensation or icing are of considerable importance in the field of collector physics, because water droplets inside a collector can cause attenuated solar yield and severe deteriorations of absorber coatings. Since nucleation is an extremely local phenomenon, general physical considerations will not suffice to predict whether condensation occurs under certain, given conditions. Therefore a detailed spatial simulation is necessary to be able to cope with this issue, i.e., a simulation based on computational fluid dynamics (CFD). This contribution describes how to incorporate the physics of classical nucleation theory (CNT), which is also briefly explained, into the open source code Open-FOAM to combine CNT with CFD. Furthermore, the results of a simple test case are included for demonstration.

1   Introduction

Condensation and ice accretion are common and important issues, also for solar thermal collectors. Humid air inside of collectors tends to condensate or sometimes even freeze on the collector glazing. Not only lead droplets or ice crystals to an attenuated solar yield through reflection and scattering of sunlight, but they can also cause severe damages when impinging on the collector coatings. This is especially inconvenient if the involved surface treatments are highly sophisticated and hence expensive. Therefore there exists the need to fully understand the conditions in the collector that lead to condensation. Ultimately, this will lead to optimized concepts of ventilation and sealing to prevent condensation while minimizing energy losses.

The path to an understanding of condensation and icing starts at practical knowledge from field studies, which stimulate experimental investigations of condensation and ice accretion (see e.g. [1–6]). The development of suitable models, in this paper through nucleation theory (see section 2), subsequently leads to investigations of the models via simulations, presented in section 3. Although there exist studies of the nucleation at surfaces on a molecular level [7], the current work does not aim at this nano-scale level, since it would be

computationally impossible to simulate and describe macroscopic devices like the interior of solar thermal collectors then.

The most detailed and still applicable method of simulation in this case is the finite volume method of computational fluid dynamics (CFD), for which there exist various commercial and free tools. Since the processes of nucleation, droplet and crystal growth and humidity transport are to be modelled, the open source code OpenFOAM [8] is used. It is open, not only in terms of source code, but also in its structure and hierarchical design, so that its solvers, utilities and libraries are fully extensible. Using these possibilities it is feasible to simulate not only the growth of films or frost layers [9], but really the physical behaviour at the onset of condensation or icing, i.e., the corresponding nucleation process, as will be shown in section 3.

2 Nucleation Theory

Nucleation is a molecular phenomenon which can (directly) only be captured by molecular dynamics simulation (c.f. [7]). To be able to perform investigations on a larger scale a suitable and widely used method is classical nucleation theory (CNT, [10]). One of its features is, that the nucleating matter is considered continuous, usually in the form of an ideal gas. Also, via the definition of the so called surface of tension (where thermodynamic and mechanical surface tension coincide), an agglomeration of water molecules is simply describable as a spherical droplet of radius r.

Even in equilibrium such a droplet is not unchanged, water molecules continuously accrete and evaporate to form a quasi–static condition. Also during nucleation processes, where the vapour pressure P_v is larger than the saturation vapour pressure $P_{v,sat}$, both these events occur, and even then it may happen that very small droplets vanish again completely. However there exists a critical size to such droplets, which depends on the surrounding conditions (see below), above which the droplets will no longer vanish but only grow further, as long as the conditions are unchanged. A droplet of this critical size is called critical embryo, quantities referring to it are subsequently labelled with a star superscript. The formation of such a critical embryo out of vapour costs (Gibbs free) energy $\Delta G^\star$ which is, according to CNT, proportional to the surface tension[*] and to the critical embryo volume $V^\star$ divided by its radius $r^\star$,

$$\Delta G^\star = \frac{\sigma V^\star}{r^\star} \,. \tag{1}$$

This formation energy represents a barrier to the nucleation process which reduces the rate J at which critical embryos occur per second per cubic meter:

$$J = J_0 \, e^{-\frac{\Delta G^\star}{k_B T}} \,, \tag{2}$$

where J_0 is the so called kinetic constant of nucleation, which also depends on material properties and surrounding conditions, $k_B = 1.3806504 \cdot 10^{-23}$ J/K is Boltzmann's constant, and T is the temperature of the embryo. The typical dependence of J on supersaturation $S - 1$ is visualized in Fig. 1(a). The supersaturation is derived from the saturation ratio $S = P_v/P_{v,sat}$ with the actual vapour pressure P_v and the saturation vapour pressure $P_{v,sat}$; S is also termed relative humidity. Clearly, the nucleation rate is extremely sensitive to supersaturation.

---

[*] $\sigma = \left(0.117 - 0.000152 \frac{T}{K}\right) \frac{N}{m}$ between water and surrounding air
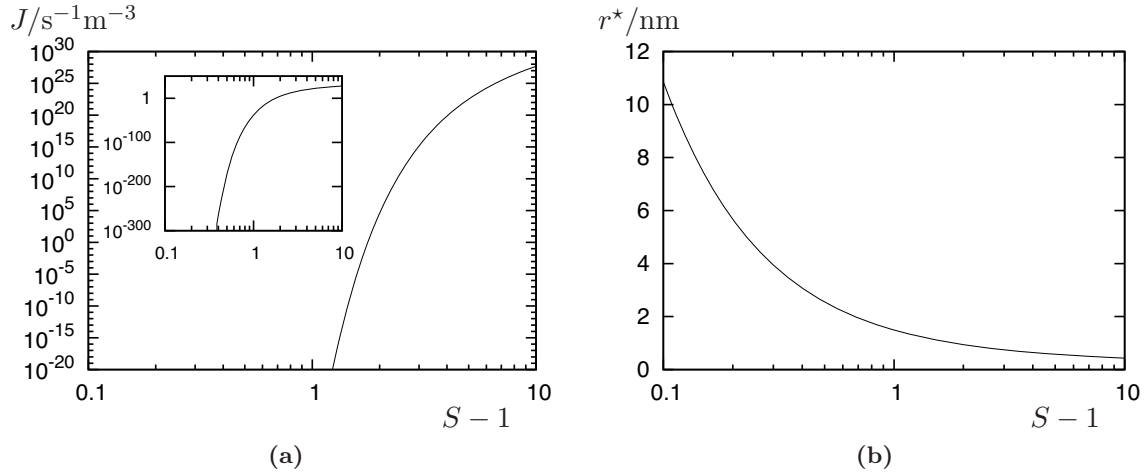
Fig. 1: Typical dependence of nucleation rate (according to the classical Becker–Döring nucleation theory) on supersaturation in panel (a) on a double logarithmic scale for $T = 300$ K. The dependence of the critical radius $r^\star$ on the supersaturation S on a single logarithmic scale for the same temperature is given in panel (b).

CNT also provides the expression for the critical embryo radius:

$$r^\star = \frac{2\sigma\mu_{H_2O}}{\rho_{H_2O}RT\ln S} \,, \tag{3}$$

where $\mu_{H_2O} = 18.0153$ g/mol is the molar mass of water, $\rho_{H_2O} = (1049.572 - 0.1763\frac{T}{K})$ kg/m^3 is the density of (liquid) water, $R = 8.314472$ J/(K mol) is the gas constant, and S is again the saturation ratio, which of course has to be larger than 1. For the saturation vapour pressure of water the relation $P_{v,sat}(T) = \exp(77.34 - 7235.42/T - 8.2\log T + 0.00571\,T)$ is used (see e.g. [10]). The dependence of $r^\star$ on the supersaturation is plotted in Fig. 1(b). For heterogeneous nucleation at a flat surface the curvature (i.e., the radius) of the critical embryo is unchanged, but the volume is lowered. Since an ideal droplet at a flat surface resembles a spherical cap, the reduced volume hence only depends on the contact angle θ. After basic geometrical considerations one obtains

$$V^\star_{het} = r^{\star 3}\frac{\pi(1 - \cos\theta)^2(2 + \cos\theta)}{3} \,, \tag{4}$$

which reduces to the homogeneous value for the completely hydrophobic surface with $\theta = \pi$. When inserting the heterogeneous critical embryo volume into Eq. (1) the same θ–dependence [see Fig. 2(a)] again occurs in the formation energy. Also, the kinetic constant of heterogeneous nucleation depends on the contact angle (a typical value would be $J_0 = 10^{26}$ m^{-2}s^{-1} [3]). Using the direct vapour deposition model [10, 11] the heterogeneous nucleation rate follows a similar trend like the homogeneous one, as can be seen in Fig. 2(b). If one makes the common choice for a critical nucleation rate (where a considerable amount of vapour condensates) of $J_{crit} = 1$ cm^{-2}s^{-1}, one can calculate, for given temperature and contact angle, the respective necessary saturation ratio. Fig. 2(c) illustrates how this critical saturation ratio varies with contact angle. The value of $S_{crit} = 1$ at $\theta = 0$ describes direct or film–like deposition of water molecules.

Of course, these considerations can easily be repeated with the surface tension of ice, but will not be included here.
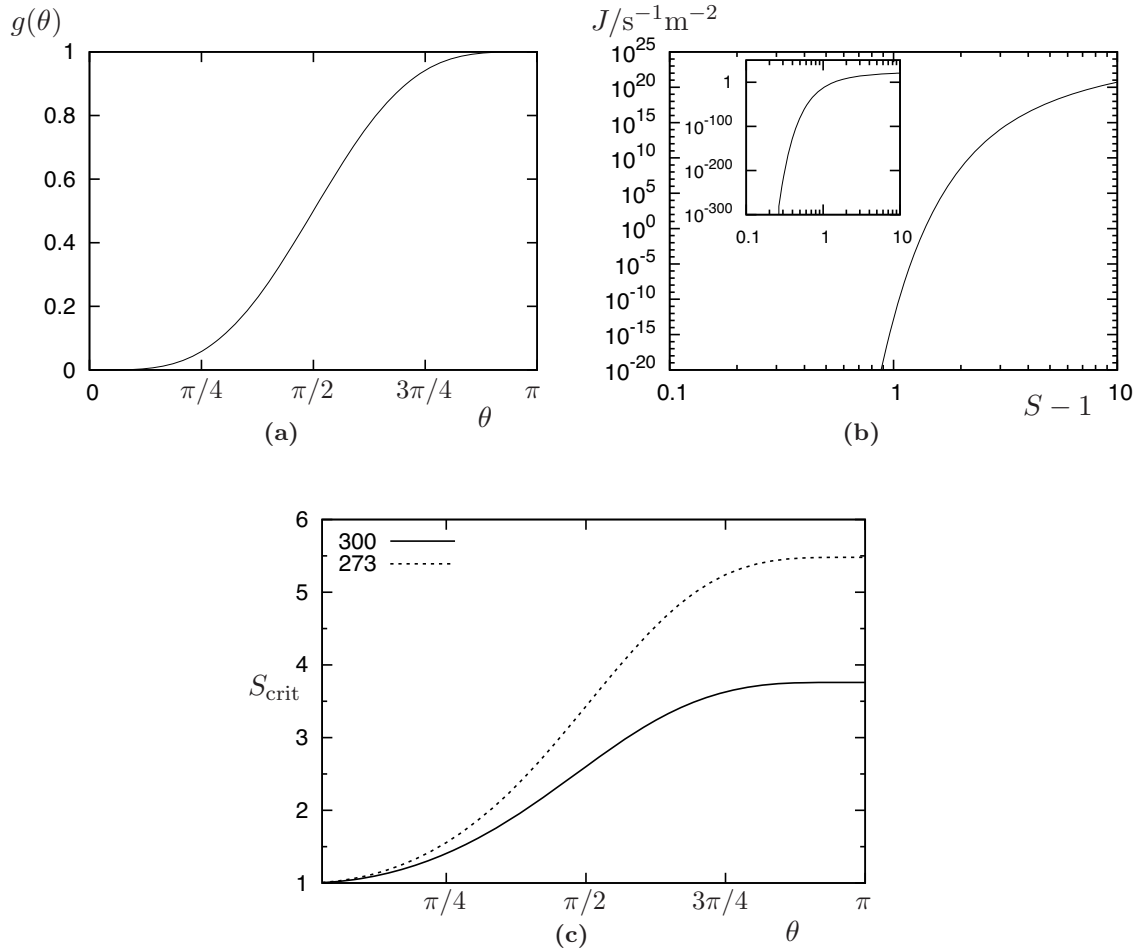
Fig. 2: The geometric factor $g(\theta) = (1-\cos\theta)^2(2+\cos\theta)/4$, relevant for the contact angle dependence of critical volume and formation energy, is plotted versus contact angle in (a). The dependence of the heterogeneous nucleation rate at $T = 300\,\mathrm{K}$ and a contact angle of $\theta = \pi/2$ on supersaturation is visualized in (b). (c) displays the critical saturation ratio in dependence of contact angle for two different temperatures, as indicated in the legend.

3 Simulations

As mentioned in section 1 it is intended to perform CFD simulations for the nucleation phenomenon of condensation. For this purpose a region similar to the test section of the experiments (see [1,2]) is set up, i.e., a rectangular duct of cross section $300\,\mathrm{mm} \times 100\,\mathrm{mm}$ and length $600\,\mathrm{mm}$. Air at $T_{\mathrm{air}} = 300\,\mathrm{K}$ and a velocity of $v = 2\,\mathrm{m/s}$ flows into the duct at one end and is exhausted against ambient pressure at the outlet. Initially it carries vapour at a mass concentration of $c_{\mathrm{m,v}} = 0.020\,\mathrm{kg/m^3}$, which is equivalent to a saturation ratio of $S = 0.8$.

As a first approach to humidity transport in air a simple scalar transport with diffusion is used for the mass concentration:

$$\frac{\partial c_{\mathrm{m,v}}}{\partial t} = -\mathrm{div}\,\mathbf{j} = \mathrm{div}\left(D_{\mathrm{v}}\,\mathrm{grad}\,c_{\mathrm{m,v}} - c_{\mathrm{m,v}}\mathbf{u}\right), \tag{5}$$

with a convective ($c_{\mathrm{m,v}}\mathbf{u}$) and a diffusive ($-D_{\mathrm{v}}\,\mathrm{grad}\,c_{\mathrm{m,v}}$) part for the vapour flux $\mathbf{j}$. The

(a)

(b)

Fig. 3: Temperature profile (a) and vapour concentration profile (b) in a plane parallel to the flow and perpendicular to the cooled surface.

used diffusion constant of vapour in air[†] is given by $D_{\mathrm{v}} \simeq 2.12 \cdot 10^{-7} \,\mathrm{m^2/s}$. In OpenFOAM[‡] this differential equation is simply introduced via two lines

```
fvScalarMatrix cmvEqn(fvm::ddt(cmv)+fvm::div(phi,cmv)-fvm::laplacian(Dv,cmv));
cmvEqn.solve();
```

and one additional variable, `cmv`, for the vapour mass concentration.

If now one of the side surfaces of the rectangular duct is cooled, i.e., held at a constant temperature $T_{\mathrm{surf}} = 273\,\mathrm{K} < T_{\mathrm{air}}$, the conditions for measurable nucleation at this surface are met. For an initial laminar simulation of the flow one quickly obtains a stable condition for flow and temperature, where the temperature profile in a plane parallel to the flow direction and perpendicular to the cooled surface has the form given in Fig. 3(a). One can clearly see the gradual cooling of the air as it flows over the cooled surface. If one also takes into account the loss of humidity due to the formation of critical embryos at the surface, there appears also a gradient in the water vapour concentration, although this change in humidity does not spread as fast as the one in temperature due to the considerably smaller (2 orders of magnitude) diffusion constant for humidity [see Fig. 3(b)].

Since the Reynolds number of the described flow condition is of the order of 10^4, a turbulent simulation is clearly necessary for a more realistic modelling of the situation. As a first step towards turbulence a standard $k - \epsilon$ model has been applied. While the profiles of temperature and vapour mass concentration are very similar in a plane like in Fig. 3, there appears, in contrast to the laminar case, a spacial peculiarity. In the region very close to the cooled surface (i.e., the first calculation layer of the flow near the surface) the humidity loss becomes much more pronounced in the corners and at the end of the rectangular duct [see Fig. 4(a)]. Fig. 4(b) gives a possible explanation for this effect: The turbulent kinetic energy k shows regions of low turbulence in the corners. The higher turbulence in the middle region may cause a better mixing of the humid air and hence a less pronounced humidity gradient.

4 Conclusion and Outlook

First steps towards a CFD simulation of nucleation phenomena have been taken and show promising results. The framework of classical nucleation theory has been extended to a model which can be incorporated into the open source CFD code OpenFOAM, which

---

[†]http://physics.holsoft.nl/physics/ocmain.htm
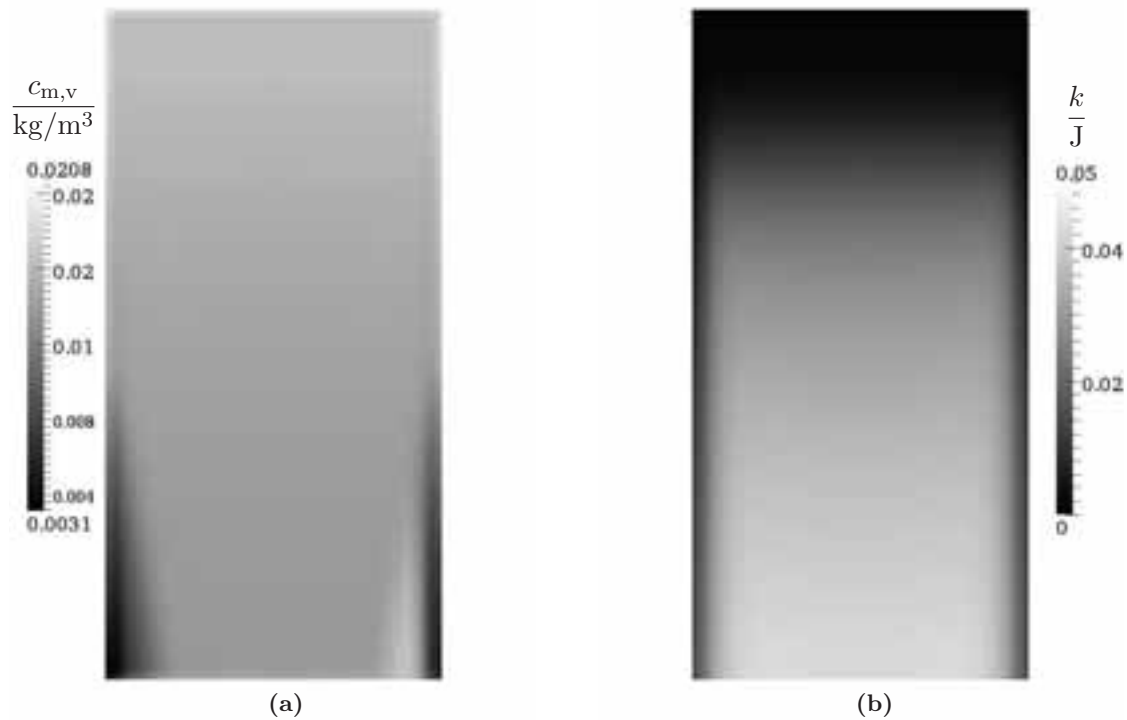[‡]http://www.openfoam.com/

Fig. 4: Vapour mass concentration (a) and turbulent kinetic energy (b) close to the cooled surface.

allows arbitrarily detailed further development. This will include the following points (in anticipated chronological order):

- Considering the influence of humidity on density and hence on the flow.

- Including gravity and hence buoyancy forces.

- Using generalized gas equations instead of the ideal gas one, for air and vapour.

- Incorporating improved nucleation rates, respecting e.g. experimental corrections like for homogeneous rates [12] or surface diffusion effects.

- Modelling the influence of turbulence on the (vapour) diffusion coefficient.

- Extending the simulations to transient conditions.

- Considering the postnucleation droplet growth [13].

- Creation of films.

- Freezing of droplets/films and growth of ice.

These investigations will finally lead to a detailed understanding of the phenomena concerning the nucleation of water vapour. But also the understanding of nucleation in general will benefit from the developed models and tools.

Acknowledgements

References

[1] Ch. Reichl, G. J. Pauschenwein, B. Windholz, B. Hebenstreit, and M. Monsberger, "Experimental studies on the icing-onset on plates in low speed flows," in *IIR 1ˢᵗ Conference on Sustainable Refrigeration and Heat Pump Technology, Stockholm* (2010).

[2] Ch. Reichl, G. J. Pauschenwein, B. Windholz, Ch. Zauner, B. Hebenstreit, M. Chouiki, and M. Monsberger, "Condensation and subsequent icing on structured plates in low speed flow – an experimental study," in *EuroSUN* (2010).

[3] R. O. Piucco, C. J. Hermes, C. Melo, and J. R. B. Jr., "A study of frost nucleation on flat surfaces," *Exp. Therm Fluid Sci*, **32**, 1710 (2008).

[4] R. D. Narhe and D. A. Beysens, "Growth dynamics of water drops on a square-pattern rough hydrophobic surface," *Langmuir*, **23**, 6486 (2007).

[5] X. Wu, W. Dai, W. Xu, and L. Tang, "Mesoscale investigation of frost formation on a cold surface," *Experimental Thermal and Fluid Science*, **31**, 1043 (2007).

[6] R. A. Shaw and D. Lamb, "Experimental determination of the thermal accommodation and condensation coefficients of water," *J. Chem. Phys.*, **111**, 10659 (1999).

[7] S. Toxvaerd, "Molecular dynamics simulation of heterogeneous nucleation at a structureless solid surface," *J. Chem. Phys.*, **117**, 10303 (2002).

[8] H. Weller, G. Tabor, H. Jasak, and C. Fureby, "A tensorial approach to computational continuum mechanics using object-oriented techniques," *Comput. Phys.*, **12**, 620 (1998).

[9] K.-S. Lee, S. Jhee, and D.-K. Yang, "Prediction of the frost formation on a cold flat surface," *Int. J. Heat Mass Tran.*, **46**, 3789 (2003).

[10] H. Vehkamäki, *Classical Nucleation Theory in Multicomponent Systems.* Berlin Heidelberg: Springer (2006). ISBN-10 3-540-29213-6, ISBN-13 978-3-540-29213-5.

[11] H. R. Pruppacher and J. D. Klett, *Microphysics of Clouds and Precipitation, Second Revised and Enlarged Edition with an Introduction to Cloud Chemistry and Cloud Electricity.* Kluwer Academic Publishers (1997).

[12] J. Wölk and R. Strey, "Homogeneous nucleation of H_2O and D_2O in comparison: The isotope effect," *J. Phys. Chem. B*, **105**, 11683 (2001).

[13] V. Pines, M. Zlatkowski, and A. Chait, "Postnucleation droplet growth in supersaturated gas with arbitrary vapor concentration," *J. Chem. Phys.*, **120**, 10455 (2004).